Anal. Chem. **2000,** *72,* 1053−1057

Electroosmotic Capillary Flow with Nonuniform Zeta Potential

A. E. Herr,* J. I. Molho, J. G. Santiago, M. G. Mungal, and T. W. Kenny

Stanford University, Stanford, California 94305-4021

M. G. Garguilo†

Sandia National Laboratories, Livermore, California 94550

The present work is an analytical and experimental study of electroosmotic flow (EOF) in cylindrical capillaries with nonuniform wall surface charge (ζ-potential) distributions. In particular, this study investigates perturbations of electroosmotic flow in open capillaries that are due to induced pressure gradients resulting from axial variations in the wall ζ-potential. The experimental inquiry focuses on electroosmotic flow under a uniform applied field in capillaries with an EOF-suppressing polymer adsorbed onto various fractions of the total capillary length. This fractional EOF suppression was achieved by coupling capillaries with substantially different ζ-potentials. The resulting flow fields were imaged with a nonintrusive, caged-fluorescence imaging technique. Simple analytical models for the velocity field and rate of sample dispersion in capillaries with axial ζ-potential variations are presented. The resulting induced pressure gradients and the associated band-broadening effects are of particular importance to the performance of chemical and biochemical analysis systems such as capillary electrokinetic chromatography and capillary zone electrophoresis.

Current benchtop biological instruments and emerging miniaturized chemical instrumentation[1,2] rely on electrokinetic mechanisms for fluid transport and sample separation in fluidic channel dimensions on the order of 10−100 micrometers. Current instruments use free-standing glass capillaries, while new miniaturized devices are fabricated on glass, quartz, silicon, or plastic substrates using techniques that originated in the semiconductor industry and the micro electromechanical systems community.[3−5] The flow phenomena in each of these devices are a complex function of the applied electric fields, the physical characteristics of the microchannels, and the physical properties of the often multicomponent fluids. Flow phenomena in continuous-flow devices are also strongly dependent on both the upstream and downstream conditions. An accurate understanding of dispersive phenomena is necessary for the design of EOF control schemes, as well as for the design of integrated microfluidic systems. The present investigation addresses this need by providing an experimental and analytical study of one important source of sample dispersion in electrokinetic systems: band broadening caused by nonuniform axial ζ-potential distributions.

Nonuniform axial ζ-potential distributions arise both accidentally and deliberately in electrokinetic systems. Microscale debris and manufacturing irregularities that may be present in microchannels introduce unknown ζ-potential distributions, as does adsorption of organics to the walls of a microchannel during analysis. Dynamic modification of the ζ-potential of a channel is inherent to certain analysis techniques; one such example is isoelectric focusing (IEF). IEF relies on the establishment of a pH gradient within a single channel. Researchers have shown that variation of solution pH has a strong effect on the ζ-potential and, hence, EOF.[6−8] The pH gradient inherent to IEF will cause nonuniform EOF in such systems.

Several researchers have investigated deliberately altering the ζ-potential in localized EOF control schemes. Towns and Regnier[8] examined situations where chemically modified capillaries (e.g., capillaries coated internally with polymers) were employed for capillary zone electrophoretic separations. Hayes and Ewing,[9] Lee et al.,[10] and Keely et al.[11] have investigated the modification of ζ-potential distributions through application of radial electric fields. Multiple capillary systems, integrated chip analysis systems, and coupled capillaries to control EOF are but a sample of other situations in which the ζ-potential of the channels would be intentionally altered.[12−15]

* Corresponding author: (phone) 650-725-1595; (fax) 650-753-3521; (e-mail) aeh@leland.stanford.edu.

† Currently at: PE Biosystems, Foster City, CA 94404.

(1) Harrison, J. D. *Science (Washington, D.C.)* **1993**, *261*, 895.
(2) Fluri, K.; Fitzpatrick, G.; Chiem, N.; Harrison, D. J. *Anal. Chem.* **1996**, *68*, 4285−4290.
(3) Ko, W. H.; Suminto, J. T. In *Sensors: A Comprehensive Survey*; Grandke, T., Ko, W. H., Eds.; VCH Press: Weinhein, Germany, 1989; Vol. 1, pp 107−168.
(4) Manz, A.; Graber, N.; Widmer, H. M. *Sens. Actuators, B* **1990**, *B1*, 244−248.
(5) Manz, A.; Fettinger, J. C.; Verpoorte, E.; Lundi, H.; Widmer, H. M.; Harrison, D. J. *Anal. Chem.* **1991**, *10*, 144−149.
(6) Lukacs, K. D.; Jorgeonson, J. W. *J. High Resolut. Chromatogr. Chromatogr. Commun.* **1985**, *8*, 407.
(7) Lambert, W. J.; Middleton, D. L. *Anal. Chem.* **1990**, *62*, 1585.
(8) Towns, J. K.; Regnier, F. E. *Anal. Chem.* **1991**, *63*, 1126−1132.
(9) Hayes, M. A.; Ewing, A. G. *Anal. Chem.* **1992**, *64*, 512−516.
(10) Lee, C. S.; Blanchard, W. C.; Wu, C. T. *Anal. Chem.* **1990**, *62*, 1550−1552.
(11) Keely, C. A.; Holloway, R. R., van de Goor, T. A. A. M.; McManigill, D. *J. Chromatogr., A* **1993**, *652*, 283−289.
(12) Manz, A.; Bessoth, F.; Kopp, M. U. Proceedings of μTAS '98, Banff, Canada, October 13−16, 1998, pp 235−240.
(13) Everaerts, F. M.; Verheggen, T. P. E. M.; van de Venne, J. L. M. *J. Chromatogr.* **1976**, *123*, 139.
(14) Towns, J. K.; Regnier, F. E. *Anal. Chem.* **1992**, *64*, 2473.

10.1021/ac990489i CCC: $19.00
Published on Web 02/01/2000

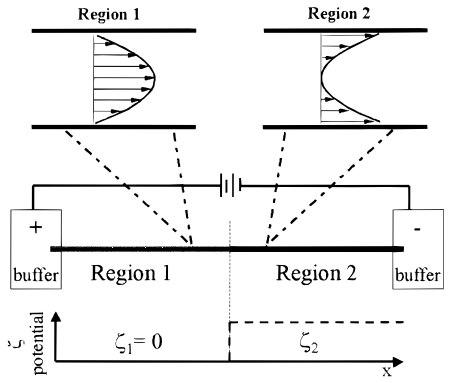

Figure 1. The schematic shows the experimental configuration that provides a step change in axial ζ-potential by coupling dissimilar capillaries. The predicted parabolic flow profile within the capillary system is depicted in the schematic. The EOF in Region 2 can be thought of as "pulling" the flow in Region 1 as continuity must be satisfied in this system. Images were collected 10 cm away from the interconnect region.

The present study characterizes scalar transport phenomena within a capillary of circular cross section using a recently developed caged-fluorescence imaging diagnostic.[16,17] An axial step change in the ζ-potential of the capillary is introduced at various distances along the length of the capillary. The effects of such ζ-potential variations are captured by imaging the scalar concentration of an optically activated fluorescent dye seeded into the flow.

THEORY

Burgreen and Nakache[18] provide a brief historical review of electrokinetic theory. Rice and Whitehead[19] give a complete analysis of electroosmotic flow in circular cross section capillaries with uniform ζ-potential, where the ζ-potential is the electric potential at the slip plane.[20] Anderson and Idol[21] developed an infinite-series solution for flow in a round capillary with an arbitrary axial ζ-potential distribution. Here we present a simplified derivation for a subset of the problems addressed by Anderson and Idol, namely electroosmotic flow in a capillary with a discrete step change in ζ-potential.

Perturbed Velocity Profile. Consider the electroosmotic flow in a capillary with a step change in ζ-potential, as illustrated in Figure 1. Let us assume that the fluid velocity is steady, fully developed and, thus, only a function of radial position in both regions of this system. Radial velocity and pressure gradients are assumed confined to a small region near the discontinuity in ζ-potential.[22] In this work, we are only concerned with the flow field far from the discontinuity. In the limit of a thin charged double-layer,[23] the expression of Rice and Whitehead,[19] applied to each region of the system depicted in Figure 1, reduces to

$$U_i(r) = \frac{-\epsilon \zeta_i E_x}{\eta} - \left(\frac{\partial P}{\partial x}\right)_i \frac{{r_0}^2}{4\eta}\left(1 - \frac{r^2}{{r_0}^2}\right) \qquad (1)$$

where U is the axial velocity, x is the axial position, ϵ is the permittivity of the buffer, η is the viscosity of the buffer, E_x is the applied axial electric field, P is the pressure, ζ is the ζ-potential, r is the radial position, and r_o is the inner radius of the capillary. The subscript i refers to a particular region of uniform ζ-potential (e.g., in Figure 1, i may equal 1 or 2).

The volumetric flow rate is found by integrating eq 1 over the cross section of the capillary for each region in Figure 1. This results in a volumetric flow rate, for each region, given by:

$$Q_i = \frac{-\epsilon \zeta_i E_x}{\eta} \pi {r_o}^2 - \left(\frac{\partial P}{\partial x}\right)_i \frac{\pi {r_o}^4}{8\eta} \qquad (2)$$

For an incompressible liquid, continuity demands that the volumetric flow rates in all regions are equal. We consider the case where the pressure at either end of the system is known (e.g., atmospheric pressure). The assumption of steady, fully developed flow in each region results in a pressure distribution that is continuous and piecewise linear. These constraints yield a readily solvable set of linear equations for the pressure gradient in each region. From these relations, the pressure gradient is

$$\left(\frac{\partial P}{\partial x}\right)_i = \frac{8E_x\epsilon}{{r_o}^2}(\bar{\zeta} - \zeta_i), \qquad (3)$$

where $\bar{\zeta} = (1/L)\sum L_i\zeta_i$ is the system average ζ-potential, with L_i and L being the length of the ith region and the total length of the coupled capillary system, respectively. On the basis of the aforementioned assumptions, eq 3 is a general result that holds for any number of step changes in ζ-potential. Combining eqs 1 and 3 gives the velocity distribution for a round capillary with axial step variations in ζ-potential:

$$U_i(r) = \frac{-\epsilon E_x}{\eta}\left[\zeta_i + 2(\bar{\zeta} - \zeta_i)\left(1 - \left(\frac{r}{r_0}\right)^2\right)\right] \qquad (4)$$

Referring to Figure 1, the velocity profiles predicted by eq 4 suggest that the EOF in Region 2 "pulls" the flow in Region 1. In other words, the EOF in Region 2 tends to create suction at the interface between the two regions and the pressure drops at the interface until the mass flow rates in each region are equal.

Both the infinite-series solution of Anderson and Idol and the treatment here result in an average velocity (i.e., volumetric flow rate divided by cross-sectional area) that is given by the Helmholtz-Smoluchowski equation based on the *average* ζ-potential:

(15) Nashabeh, W.; El Rassi, Z. *J. High Resolut. Chromatogr.* **1992**, *15*, 289−292.
(16) Lempert, W. R.; Magee, K.: Ronney, P.; Gee, K. R.; Hauglan, R. P. *Exp. Fluids* **1995**, *18*, 249−257.
(17) Paul, P. H.; Garguilo, M. G.; Rakestraw, D. J. *Anal. Chem.* **1998**, *70*, 2459−2467.
(18) Burgreen, D.; Nakache, F. R. *J. Phys. Chem.* **1964**, *68*, 1084−1091.
(19) Rice, C. L.; Whitehead, R. *J. Phys. Chem.* **1965**, *69*, 4017−4023.
(20) Hunter, R. J. *Zeta Potential in Colloid Science: Principles and Applications*; Academic Press: San Francisco, 1981.
(21) Anderson, J. L.; Idol, W. K. *Chem. Eng. Commun.* **1985**, *38*, 93−106.
(22) Long D.; Stone H. A.; Ajdari, A. *J. Colloid Interface Sci.* **1999**, *212*(2), 338−349.
(23) Probstein, R. F. *Physiochemical Hydrodynamics: An Introduction, 2nd ed.*; Wiley and Sons: New York, 1994; p 193.

$$\bar{U} = \frac{-\epsilon E_x \bar{\zeta}}{\eta} \tag{5}$$

The axial velocity component of the Anderson and Idol infinite-series solution converges to eq 4 in a region where the ζ-potential is constant or varies linearly along the axis of the capillary.[24]

Separation Efficiency. This work is primarily concerned with electroosmotic flow perturbations resulting from axial variations in the ζ-potential. However, the analysis and experiments presented here are directly applicable to studies of sample dispersion. A pressure-driven fluid flow superposed upon a bulk "pluglike" electrokinetic velocity will cause sample dispersion and, hence, loss of sample definition.[24−27] Taylor[28] has described the sample variance caused by a pressure-driven flow as:

$$\sigma^2 = 2Dt + 2\left(\frac{r_o{}^2 \overline{U^2}_{\text{pressure}}}{48D}\right) t \tag{6}$$

where r_o is the capillary radius, $\bar{U}_{\text{pressure}}$ is the average pressure-driven velocity, t is the time since sample injection, and D is the diffusion coefficient. This variance will hereafter be referred to as the dispersion of the sample. The time rate of change of this quantity will be called the dispersion rate. In the present case, $\bar{U}_{\text{pressure}} = \epsilon E_x(\zeta_i - \bar{\zeta})/\eta$. Differentiating eq 6 with respect to time and dividing by 2D gives the ratio of the total dispersion rate to the dispersion rate due to diffusion alone:

$$\frac{\dot{\sigma}^2}{\dot{\sigma}_{\text{diff}}{}^2} = 1 + \frac{r_0{}^2\left(\frac{\epsilon E_x(\zeta_i - \bar{\zeta})}{\eta}\right)^2}{48D^2} \tag{7}$$

Equation 7 shows that the local dispersion rate (and therefore the local contribution to long-term sample dispersion) increases as the square of the difference between the local and average ζ-potentials. Equation 7 will be used to discuss the relative dispersion rates observed in the present study. Recall that this description is valid when the ζ-potential varies axially in discrete jumps and only applies at locations several diameters away from a jump in ζ-potential. To calculate the dispersion rate or dispersion for an arbitrary ζ-potential distribution, one must use the method of Datta and Kotamarthi.[26]

EXPERIMENTAL SECTION

Chemicals. A caged 5-(and 6)-carboxy-Q-rhodamine, succinimidyl ester dye purchased from Molecular Probes was used for the present investigation. A buffer solution of 50% acetonitrile (Aldrich Corp.) and 50% 5 mM tris (hydroxymethyl) aminomethane (TRIS) (Sigma Corp.) at a pH of 8.1 was used. The acetonitrile was used to aid the dissolution of the dye into the buffer. One milligram of the dye was mixed with 1 mL of the buffer solution and then sonicated for 20 min. The resulting solution was filtered through a 0.2-micrometer filter prior to injection into the coupled capillary systems. While not in use, all solutions were stored in a dark, cool place to minimize uncaging.

Coupled-Capillary System. To demonstrate how variations in the axial ζ-potential of a microchannel affect an electroosmotic flow under a uniform applied field, we examined electroosmotic flows in fused-silica capillaries with an EOF-suppressing polymer adsorbed onto various fractions of the total capillary length, as depicted in Figure 1. These capillaries were coated internally with a proprietary material and were purchased from Supelco. Their internal and external diameters are 75 and 360 μm, respectively. The transparent, bare fused-silica capillaries were purchased from Polymicro Technologies, Inc. and had similar internal and external diameters to those of the coated capillaries.

At pH 8.1, this coupled-capillary arrangement produced a coated region with a suppressed ζ-potential and a bare fused-silica region with a net negative ζ-potential. The capillary ends were cleaved and butted together within a Teflon sleeve. Each system was visually inspected for liquid leakage and flow blockage. The total length of the coupled capillary pair was maintained at 50 cm with an applied electric field strength of 100 V/cm for all cases unless otherwise noted.

The EOF-suppressing capillaries used were fabricated with an opaque polyimide coating on their outer surface. Therefore, the imaging was conducted on the transparent bare fused-silica fraction of the coupled capillary length—the EOF-supporting region. Premanufactured windows (i.e., transparent regions approximately 5 mm in length) were available on some of the EOF-suppressing capillaries and, when possible, images were acquired at these locations as well. New windows were not created with the usual method of thermowire stripping because of the concern of thermal damage to the interior EOF-suppressing polymer coating.

Imaging Diagnostics and Acquisition. Originating with the work of Lempert et al.,[16] the caged-fluorescence flow diagnostic employed in this study has been modified for microscale systems by Paul et al.[17] Like traditional dye injection techniques, the caged-fluorescence technique allows optical extraction of information about scalar transport in microfluidic systems. A caged dye was homogeneously distributed throughout a buffer solution and then injected into the coupled-capillary system. To obtain concentration information, the buffer was excited to fluoresce through two independent laser-excitation events: (1) an uncaging of the dye and (2) the application of fluorescence-exciting illumination. A time sequence of independent realizations was then obtained and processed. The details of this procedure have recently been described in the work of Paul et al.[17] The caged-fluorescence method is especially useful in flow-field interrogation, as the technique essentially allows an "optical injection" of a well-defined sample plug. This eliminates any initial sample distortion that would be created through the physical injection of dye by hydrodynamic and electrokinetic means.

The coupled-capillary system was secured to a three-axis stage by a magnetic clamping system. The fused-silica capillary itself was sandwiched between two glass microscope slide covers, and the viewing region of the system was submerged in a liquid with a matching index of refraction (refractive index = 1.47) to reduce

(24) Keely, C. A.; van de Goor, T. A. A. M.; McManigill, D. *Anal. Chem*. **1994**, *66*, 4236−4242.
(25) Wu, C.-T.; Huang, T.-L.; Lee, C. S.; Miller, C. J. *Anal. Chem*. **1993**, *65*, 568−571.
(26) Datta, R.; Kotamarthi, V. R. *AIChE J.* **1990**, *36*, 916−926.
(27) Grushka, E. *J. Chromatogr*. **1991**, *559*, 89.
(28) Taylor, G. I. *Proc. R. Soc. London, Ser. A* **1953**, *CCXIX*, 186−203.

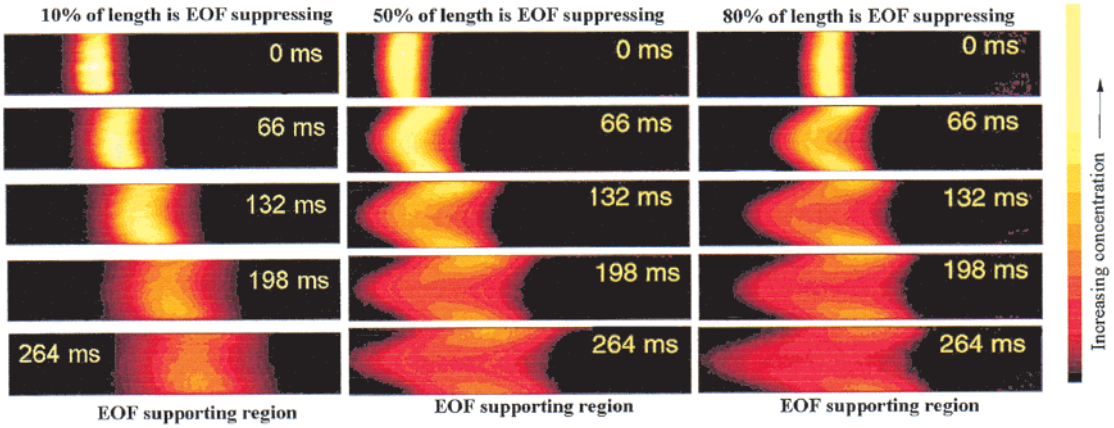

Figure 2. This figure shows experimental data generated from the apparatus shown in Figure 1. Each column represents a different coupled-capillary system, 10%, 50%, and 80% EOF suppression (left to right), with rows representing the time elapsed since the initial uncaging event. Note the parabolic shape of the dye packet, which becomes more pronounced as fractional EOF suppression increases. Experimental conditions: field strength 100 V/cm (positive from left to right), 360-o.d./75-i.d. (μm); total length of coupled-capillary system, 50 cm. Images were collected 10 cm away from the interconnect region.

image distortion due to the curvature of the capillary. Each capillary end was submerged in a buffer reservoir. Using height-adjustable stages, the reservoirs were leveled to eliminate any pressure head created by a height difference between the two reservoirs. Platinum electrodes were inserted into the reservoirs to supply the high voltage necessary for the electroosmotic flow. Prior to initiation of the electroosmotic flow, a time sequence of images was collected to verify that no pressure-driven flow existed due to a height difference between the reservoirs.

RESULTS AND DISCUSSION

In an effort to capture the effects of an axial variation in ζ-potential on the electrokinetic velocity profiles, flows were imaged in the coupled-capillary systems described above. Systems representing 10, 50, 66, and 80% EOF-suppressing fractions were investigated. These flows were imaged on the EOF-supporting bare fused silica capillary region of the coupled-capillary system.

A series of control experiments were also conducted to isolate any scalar transport distortion effects arising strictly from the presence of the Teflon interconnect. In these experiments, two bare fused silica capillaries (no EOF suppression) were joined in the same manner as the coupled-capillary systems described previously. Small dispersive effects were observed in the control cases, but this dispersion was less than that introduced by the ζ-potential variation seen in the test cases. Thus, when the fraction of EOF suppression exceeds 10%, the dispersion introduced by the interconnect is insignificant when compared with the dispersion due to the induced pressure-driven flow component. Analytical models, such as those presented by Grushka et al.,[29] suggest that thermal effects due to Joule heating are negligible in the cases presented here.

Figure 2 shows the increase of sample dispersion, in the EOF-supporting region, associated with the increasing fraction of EOF suppression. The first image in each column corresponds to the initial uncaging event. The width of this initial dye mark is approximately 25 μm. Note the parabolic shape of the dye mark as time progresses. This parabolic shape, characteristic of a pressure-driven flow, becomes more pronounced as the EOF-suppression fraction increases.

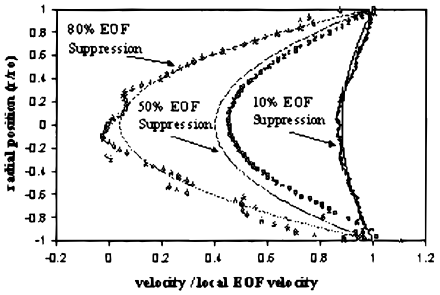

Figure 3. Comparison of scalar velocity distributions predicted by eq 4 using 40% active silanol groups in the EOF-suppressing region (solid lines) with those extracted from the data (solid points). In total, six trials of each configuration were conducted. Results from these trials have the same trends as the data presented in this figure.

A comparison of our experimental data to analytical velocity profiles, assuming one-dimensional, fully developed flow, is displayed in Figure 3. To estimate the flow velocities from the data, we fit the scalar intensity of each image row with a Gaussian curve. The maxima of the Gaussian distributions were then tracked in time, yielding the scalar velocity at each radial position. Note that the dye experiences an electrophoretic velocity that was subtracted to obtain the velocity of the buffer. The actual amount of EOF suppression in the coated region was used as an adjusted parameter when matching the theory to the experimental data.[30] Figure 3 shows the prediction based upon 40% active silanol groups in the EOF-suppressing region. This prediction is in good agreement with the velocity data for the various cases considered. The empirical evidence demonstrates that increasing the percentage of EOF-suppressing length increases the amount of pressure-driven flow in the EOF-supporting region. The measured velocity profiles provided by the current experiments should also be useful in validating numerical models that seek to capture full scalar and velocity fields. Such spatial information is not available from studies that rely upon single-point detection (e.g., UV absorption).

(29) Grushka, E.; McCormick, R. M.; Kirkland, J. J. *Anal. Chem.* **1989**, *61*, 241.

(30) Huang, T.-L.; Tsai, P.; Wu, C.-T.; Lee, C. S. *Anal. Chem.* **1993**, *65*, 2887–2893.

Equation 7 predicts that the sample-dispersion rate will increase as the difference between the local ζ-potential and the average ζ-potential increases. The dispersion rate ratio, $\dot{\sigma}^2/\dot{\sigma}^2_{\text{diff}}$, was calculated using eq 7 and the extracted velocity data presented in Figure 3. This ratio is 1.1, 4.0, and 8.7 for the 10, 50, and 80% EOF-suppression cases, respectively. The local ζ-potential is negative and the same value for the three cases presented in Figure 2. However, the average ζ-potential increases as the fraction of EOF-suppressing length increases. As predicted, the dispersion rate in the EOF-supporting region *increases monotonically* as the percentage of EOF-suppressing length increases.

As previously defined in the Theory section, the local dispersion-rate ratio (eq 7) is the ratio of the dispersion rate due to the local velocity profile and diffusion normalized by the dispersion rate due to diffusion alone. Multiplying both the numerator and denominator by an elution time (multiplying by unity) gives a ratio of total dispersions, and therefore, the dispersion rate ratio can also be thought of as a total dispersion ratio. Note, however, that, to calculate the total dispersion ratio arising in a given separation system (i.e., between an injector and the corresponding detector), one must calculate the average value of eq 7 as the sample travels through that system. If the injector and detector were contained within Region 1 of Figure 1, while the electrodes remained at either end of the coupled-capillary system, the total dispersion ratio will simply be eq 7 evaluated in Region 1. This configuration is similar to the system presented by Nashabeh and El Rassi.[15] If, however, the injector and detector are at either end of the entire coupled-capillary system, then the total dispersion ratio is a weighted average of eq 7 in each region of the system (neglecting the additional dispersion caused at the interface between the two regions). In this case, the total dispersion ratio is maximized when the coupled-capillary system is 50% EOF-suppressing and 50% EOF-supporting.

Figure 4 shows a series of additional images collected in the EOF-suppressing region and the corresponding EOF-supporting region (seen through the premanufactured windows) for a capillary with 66% fractional EOF suppression. These images show that the direction of the pressure-driven velocity is different in each of the two regions, as predicted by eq 4 and schematically depicted in Figure 1. In this case, the ζ-potential in the EOF-supporting region is more negative than the average ζ-potential, so the induced pressure-driven flow acts against the electric field in this region. In the EOF-suppressing region, the ζ-potential is greater than the average ζ-potential, so the induced pressure-driven flow is in the same direction as the electric field. Chien and Helmer[31] observed similar behavior in a capillary system with an axially varying electroosmotic velocity. In that work, they investigated buffers of mismatched concentration in a field-amplified capillary electrophoresis system. Figure 4 demonstrates that flow phenomena at a given location in a continuous-flow device are sensitive to both the upstream and downstream conditions.

(31) Chien, R.-L.; Helmer, J. C. *Anal. Chem.* **1991**, *63*, 1354−1361.

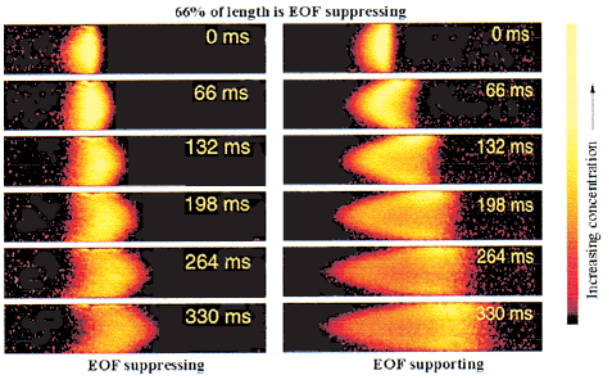

Figure 4. Experimental data obtained from a coupled capillary system where 66% of the total system length was EOF-suppressing. Images were collected in both the EOF-suppressing (image sequence on left) and EOF-supporting regions (image sequence on right) of this single coupled system. Note the complementary nature of the flow profiles, as described in the caption of Figure 1. Experimental conditions: field strength, 84 V/cm (positive from left to right); 360-o.d./75-i.d. (μm); total length of coupled-capillary system, 30 cm.

CONCLUSIONS

This paper has presented an analytical and experimental study of EOF in cylindrical capillaries with a discrete change in ζ-potential. This ζ-potential distribution allows a straightforward derivation of a simple model for the fluid velocity and sample-dispersion rate. The experimental study utilized a recently developed caged-fluorescence technique to extract information about the fluid velocity and sample-dispersion rate. These measurements also provide data that could be used to verify numerical efforts. Empirical evidence was presented showing that the dispersion rate in an EOF-supporting region increases monotonically as the length of EOF-suppressing capillary increases. More generally, the model and experimental results confirm that, at a given location in the capillary system, the velocity profile and sample-dispersion rate are a function of the local ζ-potential *and* system-average ζ-potential.

ACKNOWLEDGMENT

The authors gratefully acknowledge Sandia National Laboratories' Laboratory-Directed Research and Development Program (Livermore, CA). We also thank P. H. Paul and D. J. Rakestraw of Sandia National Laboratories (Livermore, CA), J. Gilbert and M. Deshpande at Microcosm, and P. M. St. John at PE Biosystems. Financial support was partially supplied by DARPA (Composite CAD Grant no. F30602-96-0306). A.E.H. and J.I.M. were funded by the National Science Foundation's Graduate Research Fellowship Program and Stanford University and Hewlett-Packard's Graduate Fellowship Program, respectively.

Received for review May 6, 1999. Accepted November 30, 1999.

AC990489l